PROCEEDINGS OF SCIENCE

Diamond detector technology: status and perspectives

The RD42 Collaboration

A. Alexopoulos[3], M. Artuso[22], F. Bachmair[26], L. Bäni[26], M. Bartosik[3], J. Beacham[15], H. Beck[25], V. Bellini[2], V. Belyaev[14], B. Bentele[21], E. Berdermann[7], P. Bergonzo[13], A. Bes[30], J-M. Brom[9], M. Bruzzi[5], M. Cerv[3], G. Chiodini[29], D. Chren[20], V. Cindro[11], G. Claus[9], J. Collot[30], J. Cumalat[21], A. Dabrowski[3], R. D'Alessandro[5], W. de Boer[12], B. Dehning[3], C. Dorfer[26], M. Dunser[3], V. Eremin[8], R. Eusebi[27], G. Forcolin[24], J. Forneris[17], H. Frais-Kölbl[4], K.K. Gan[15], M. Gastal[3], C. Giroletti[19], M. Goffe[9], J. Goldstein[19], A. Golubev[10], A. Gorišek[11], E. Grigoriev[10], J. Grosse-Knetter[25], A. Grummer[23], B. Gui[15], M. Guthoff[3], I. Haughton[24], B. Hiti[11], D. Hits[26], M. Hoeferkamp[23], T. Hofmann[3], J. Hosslet[9], J-Y. Hostachy[30], F. Hügging[1], C. Hutton[19], H. Jansen[3], J. Janssen[1], H. Kagan*[15], K. Kanxheri[31], G. Kasieczka[26], R. Kass[15], F. Kassel[12], M. Kis[7], G. Kramberger[11], S. Kuleshov[10], A. Lacoste[30], S. Lagomarsino[5], A. Lo Giudice[17], E. Lukosi[28], C. Maazouzi[9], I. Mandic[11], C. Mathieu[9], N. McFadden[23], M. Menichelli[31], M. Mikuž[11], A. Morozzi[31], J. Moss[15], R. Mountain[22], S. Murphy[24], M. Muškinja[11], A. Oh[24], P. Oliviero[17], D. Passeri[31], H. Pernegger[3], R. Perrino[29], F. Picollo[17], M. Pomorski[13], R. Potenza[2], A. Quadt[25], A. Re[17], M. Reichmann[26], G. Riley[28], S. Roe[3], D. Sanz[26], M. Scaringella[5], D. Schaefer[3], C.J. Schmidt[7], S. Schnetzer[16], T. Schreiner[4], S. Sciortino[5], A. Scorzoni[31], S. Seidel[23], L. Servoli[31], B. Sopko[20], V. Sopko[20], S. Spagnolo[29], S. Spanier[28], K. Stenson[21], R. Stone[16], C. Sutera[2], A. Taylor[23], M. Traeger[7], D. Tromson[13], W. Trischuk[18], C. Tuve[2], L. Uplegger[6], J. Velthuis[19], N. Venturi[18], E. Vittone[17], S. Wagner[21], R. Wallny[26], J.C. Wang[22], J. Weingarten[25], C. Weiss[3], T. Wengler[3], N. Wermes[1], M. Yamouni[30], M. Zavrtanik[11]

PoS(Vertex 2016)027

[1] *Universität Bonn, Bonn, Germany,*
[2] *INFN/University of Catania, Catania, Italy,*
[3] *CERN, Geneva, Switzerland,*
[4] *FWT, Wiener Neustadt, Austria,*
[5] *INFN/University of Florence, Florence, Italy,*
[6] *FNAL, Batavia, USA,*
[7] *GSI, Darmstadt, Germany,*
[8] *Ioffe Institute, St. Petersburg, Russia,*
[9] *IPHC, Strasbourg, France,*
[10] *ITEP, Moscow, Russia,*
[11] *Jožef Stefan Institute, Ljubljana, Slovenia,*
[12] *Universität Karlsruhe, Karlsruhe, Germany,*
[13] *CEA-LIST Technologies Avancees, Saclay, France,*
[14] *MEPHI Institute, Moscow, Russia,*
[15] *The Ohio State University, Columbus, OH, USA,*
[16] *Rutgers University, Piscataway, NJ, USA,*
[17] *University of Torino, Torino, Italy,*
[18] *University of Toronto, Toronto, ON, Canada,*
[19] *University of Bristol, Bristol, UK,*
[20] *Czech Technical Univ., Prague, Czech Republic,*
[21] *University of Colorado, Boulder, CO, USA,*
[22] *Syracuse University, Syracuse, NY, USA,*
[23] *University of New Mexico, Albuquerque, NM, USA,*
[24] *University of Manchester, Manchester, UK,*
[25] *Universität Goettingen, Goettingen, Germany,*
[26] *ETH Zürich, Zürich, Switzerland,*
[27] *Texas A&M, College Park Station, TX, USA,*
[28] *University of Tennessee, Knoxville, TN, USA,*
[29] *INFN-Lecce, Lecce, Italy,*
[30] *LPSC-Grenoble, Grenoble, France,*
[31] *INFN-Perugia, Perugia, Italy*
E-mail: kagan.1@osu.edu

The status of material development of poly-crystalline chemical vapor deposition (CVD) diamond is presented. We also present beam test results on the independence of signal size on incident particle rate in charged particle detectors based on un-irradiated and irradiated poly-crystalline CVD diamond over a range of particle fluxes from 2 kHz/cm^2 to 10 MHz/cm^2. The pulse height of the sensors was measured with readout electronics with a peaking time of 6 ns. In addition the first beam test results from 3D detectors made with poly-crystalline CVD diamond are presented. Finally the first analysis of LHC data from the ATLAS Diamond Beam Monitor (DBM) which is based on pixelated poly-crystalline CVD diamond sensors bump-bonded to pixel readout electronics is shown.

The 25th International workshop on vertex detectors
September 26-30, 2016
La Biodola, Isola d'Elba, ITALY

*Speaker.

1. Introduction

At present most experiments at the CERN Large Hadron Collider (LHC) are planning upgrades in the next 5-10 years for their innermost tracking layers as well as their luminosity monitors in order to be able to take data as the luminosity increases and CERN moves toward the High Luminosity-LHC (HL-LHC) [1]. These upgrades will require detectors with radiation tolerance up to a total fluence of $\sim 2 \times 10^{16}$ hadrons/cm^2. This requirement is driving all LHC experiments to undertake intense research programs in radiation tolerant sensor technologies and geometries. Chemical Vapor Deposition (CVD) diamond has been used extensively and successfully in beam conditions/beam loss monitors as the innermost detectors in the highest radiation areas of essentially all LHC experiments [2],[3],[4]. As a result, CVD diamond is considered a candidate technology for beam conditions/beam loss monitors and possibly tracking layers very close to the interaction region of the LHC upgrades where the most extreme radiation conditions will exist.

The RD42 collaboration at CERN is leading the effort to develop radiation tolerant devices based on poly-crystalline CVD (pCVD) diamond as a material for tracking detectors operating in harsh radiation environments. During the last three years the RD42 group has succeeded in producing and measuring a number of devices to address specific issues related to use at the HL-LHC. This paper presents the status of the RD42 project with emphasis on recent beam test results. In particular results are presented on new material development, on the independence of signal size on incident particle rate in pCVD diamond detectors over a range of particle fluxes up to 20 MHz/cm^2 and on the 3D detector geometry where the first pCVD 3D detectors produced were shown to collect nearly all of the charge deposited in the material and are expected to be extremely radiation tolerant devices. The startup of the LHC in 2015 brought a new milestone for diamond detector development where the first planar diamond pixel modules based on pCVD diamond bump-bonded to FE-I4 ASICs [5] were installed in the ATLAS experiment[6] (the ATLAS Diamond Beam Monitor [7],[8]) and successfully began taking data.

2. Material Development

One of the focus areas of the RD42 program is the characterization of diamond material. The goal is to provide diamond manufacturers with feedback to enhance the quality of the material produced. Over the years this program has yielded dramatic results. The diamond material used in the construction of the ATLAS DBM in 2013 was 500μm thick and had a charge collection distance (CCD: the mean distance the electron-hole pairs move apart under the influence of an applied electric field) of 200-225μm and an initial uniformity of 25% causing extensive selection procedures to be necessary to secure enough material for the project. Since the DBM project, production capabilities have been expanded, higher quality material has been produced and the uniformity has dramatically increased. At present, routine wafer production yields 500μm thick parts with charge collection distance of 300-325μm starting from an initial uniformity of 5%. Moreover the understanding of the growth process has been expanded to the extent that the manufacturers are striving to reach a 400μm CCD in a 500μm thick production part.

3. Rate study of poly-crystalline CVD detectors at PSI

In order to study the dependence of signal size on incident particle rate, RD42 performed a series of beam tests in the πM1 beam line of the High Intensity Proton Accelerator (HIPA) at Paul Scherrer Institute (PSI). This beam line is able to deliver 260 MeV/c π^+ fluxes from a rate of $\sim$5 kHz/cm^2 to a rate $\sim$20 MHz/cm^2 in bunches spaced 19.8ns apart [9].

Last year RD42 published the results of rate studies up to 300 kHz/cm^2, showing that the pulse height in diamond detectors was independent of flux up to these rates [10]. This year this study was extended up to 10 MHz/cm^2. In order to extend the rate studies new front-end electronics based on a CERN fast amp [11] was designed which, when connected to a detector with $\sim$ 2 pf capacitance, has a peaking time of $\sim$6 ns, a return-to-baseline in $\sim$18 ns and 550 e noise. Sensors made from pCVD material [12] were tested in a beam telescope [13] based on 100 μm $\times$ 150 μm pixel sensors readout by the PSI46v2 pixel chip [14]. As in the original test the amplified signals were recorded with a DRS4 evaluation board [15] operating at 2 GS/s. The entire system was triggered with a scintillator which determined the timing of the beam particles with a precision of $\sim$0.7 ns.

Figure 1 shows a single DRS4 trace of a typical diamond signal for a minimum ionizing particle. For each triggered event the signal was measured at a fixed time (69 ns) after the scintillator trigger by averaging the waveform in the 10 ns window labeled "peak" in Fig. 1. Likewise the pedestal was measured in the window one bunch (19.8 ns) before the mean signal time by averaging the waveform in the 10 ns window, labeled "pedestal" and indicated in Fig. 1.

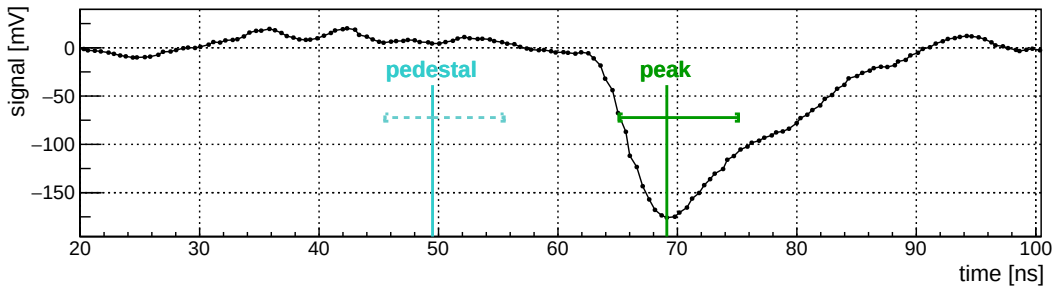

Figure 1: A sample signal trace. The horizontal bars indicate the regions where pedestal (dashed) and signal (solid) were calculated.

A series of cuts were applied to the data. These include removing 60s of seconds of triggers at the beginning of each run, removing triggers from heavily ionizing particles with saturated waveforms (mostly protons), removing calibration triggers, removing triggers in the wrong beam bucket, removing triggers with no tracks in the telescope and removing triggers with large angle tracks in the telescope. After applying this procedure all telescope tracks which project into the diamond fiducial region have a pulse height well separated from the pedestal distribution in the diamond i.e. the diamond is 100% efficient at all rates. The same procedure was applied to all particle flux points and the resulting mean pulse height versus rate is shown in Fig. 2.

The uncertainty on the data points in the plot include both statistical and systematic sources. The systematic uncertainty was determined by assuming any deviations in pulse height for rates

below 80 kHz/cm^2 was due to systematic effects. Under this assumption (which is consistent with source measurements), the standard deviation of the distribution of the average pulse height measurements for all flux points below this flux was used as the estimate of the systematic uncertainty.

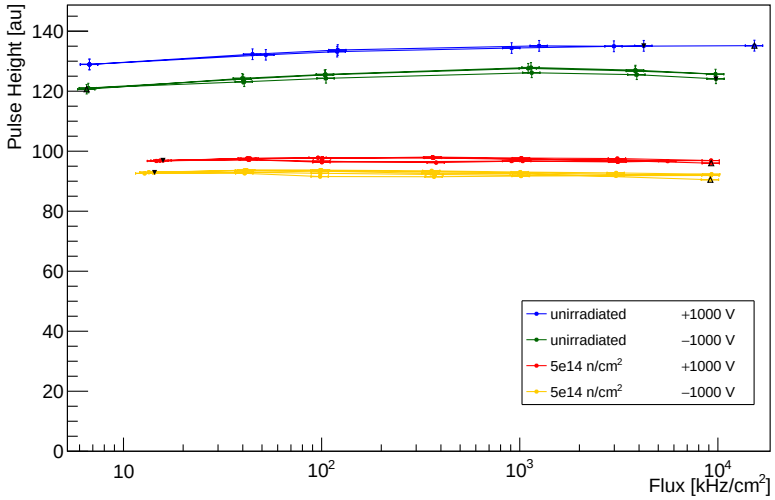

Figure 2: Average pulse height versus rate for an un-irradiated and irradiated ($5\times$ 10^{14} n/cm^2) pCVD diamond pad detector at positive and negative voltage. The pulse height units are arbitrary and the un-irradiated and irradiated detectors used different readout electronics. The resulting electronics gain corrections and the relative gain correction for the different signal direction (positive versus negative signals) in the electronics is still being determined and has not been applied.

4. 3D diamond detector beam tests at CERN

3D sensors with electrodes in the bulk of the sensor material were first proposed by Parker, *et al.* [16] in 1997 in order to reduce the drift distance of the charged carriers to less than the sensor thickness. This is particularly beneficial in detectors with a limited mean free path such as trap dominated sensor materials like heavily irradiated silicon and poly-crystalline diamond. Last year RD42 published results of a 3D device fabricated in single-crystal CVD diamond [17]. This year we fabricated the first 3D device in poly-crystalline diamond. The electrodes in the bulk of the 3D diamond device were fabricated with lasers as described in [17]. The bias electrodes were placed at the corners and the readout electrodes were placed in the middle of the cells.

For the first 3D device in pCVD material a 5mm $\times$ 5mm $\times$ 525μm diamond was used [12]. The metalization combined three different patterns on one pCVD diamond: a planar strip detector with 50 μm strip pitch operated at 500 V, a 3D detector with electrodes in the bulk forming 150μm $\times$ 150μm cells connected with metal strips to either the readout electrodes or the bias electrodes operated at 60 V and a 3D phantom with the same metalization pattern as the 3D detector but without any bulk electrodes also operated at 60 V. Fig. 3a) shows a photograph of the finished device and Fig. 3b) shows the metalization mask pattern.

In order to improve the contact with the resistive columns and thereby increase the number of working cells the same metalization pattern was put on both top and the bottom of the 3D and

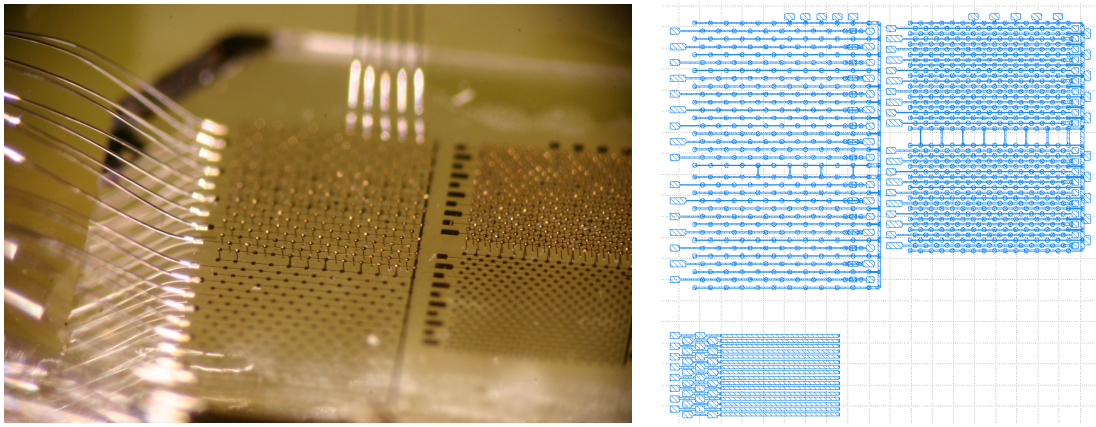

(a) Photo of the 3D device showing the metalization pattern

(b) Metalization mask

Figure 3: a)Photograph of the 3D device and b)drawing of the metalization mask. The test device consists of 3 detectors: a planar strip detector with a 50μm strip pitch operated at 500 V (b, bottom left), a 3D detector connected by a metal strip to either readout or bias detector operated at 60 V (b, top left) and a 3D phantom detector (b, middle left), where the 3D detector metalization pattern was used but with no bulk electrodes operated at 60 V. The structures (b, top right) and (b, middle right) were not connected for this test.

the phantom devices while the planar pattern received a pad metalization on the back side. The details of the fabrication are similar to the device described in [17], where additional details on the fabrication may be found.

The metalized sensor was wire-bonded to a VA2 readout chip[18]. The completed detector was then installed into a high resolution beam telescope in the H6A secondary beam line of SPS complex at CERN. The beam line was tuned to provide a 120 GeV/c positive beam with an average flux of $\sim$30 kHz/cm^2. The pulse height of the beam particles in the detector was measured for both positive and negative bias voltages. In order to assess the performance of the detector, the noise of every connected channel was measured in the events in which there was no hit on that channel. The width of the pedestal distribution yields the noise on a given channel. The average noise of the planar device was measured to be 80 e, of the 3D phantom device to be 82 e and in the 3D device to be 94 e after removing two noisy strips. This roughly scales like the capacitance of the devices. In total 16 planar strips, 9 ganged columns from the 3D phantom and 7 ganged columns from the 3D detector were used in the analysis. After reconstructing hits in the telescope and the 3D device the first 10% of the events were used for alignment. The rest of the events were then used in the analysis. Tracks were projected into the plane of the diamond and the average pulse height in the diamond was calculated with respect to the predicted hit position.

In order to disentangle the column production efficiency from the 3D detector performance and compare it to the planar strip device, a continuous fiducial region of working cells was selected (Fig. 4a). The pulse height spectrum of the 3D detector fiducial region and the pulse height spectrum of the strip detector are shown in Fig. 4b. The average charge collected by the 3D device is about twice as large as that of the strip detector. Recently the RD42 group has achieved three

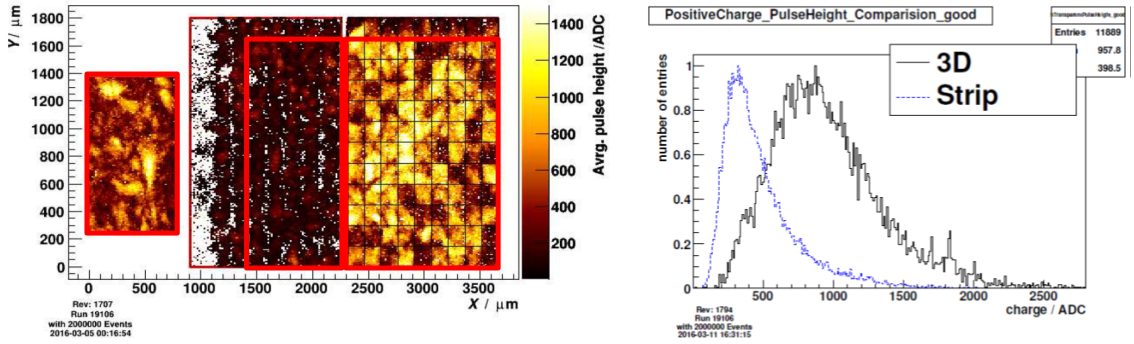

(a) (b)

Figure 4: a) Average pulse height versus predicted hit position in the strip, 3D phantom and 3D pattern (from left to right) b) Pulse height distributions of the 3D detector in the fiducial region of (a) (marked in green) compared with the pulse height distribution of the strip detector measured with the same electronics on the same diamond.

dramatic improvements in 3D device fabrication: an order of magnitude larger structures (1188 vs 99 3D cells), smaller cell size (100μm vs 150μm cells) and higher column production efficiency (99% vs 92%). After these improvements a new pCVD 3D detector was fabricated and measured in the same beam line as above. The data are being analyzed. Preliminary results indicate (in a 10% contiguous region of this device) a mean pulse height approaching ∼85% of full charge collection for a corresponding thickness. This represents the largest charge observed with a pCVD diamond detector, confirming the potential of the 3D pattern technique for diamond sensors.

5. The ATLAS Diamond Beam Monitor

The ATLAS Diamond Beam Monitor (DBM) is the first installed diamond pixel detector in a high-energy physics experiment. Its purpose is to measure instantaneous luminosity, background rates and the beam spot position. A single DBM module consists of a 18 mm $\times$ 21 mm pCVD diamond 500 μm thick instrumented with the FE-I4 pixel chip. The 26,880 pixels are arranged in 80 columns on 250 μm pitch and 336 rows on 50 μm pitch resulting in an active area of 16.8 mm $\times$ 20.0 mm. This fine granularity was designed to provide high precision particle tracking. Moreover, with the Time-over-Threshold measurement the deposited charge from a particle can be determined.

The DBM diamond module production (flip chip to FE-I4, assembly by gluing and wire-bonding) was mainly performed during the LHC long shutdown in 2013-2014. The DBM uses diamonds with a CCD of 200-220 μm at an applied bias voltage of 500 V. Three telescopes (plus 1 telescope with silicon sensors) each with 3 diamond DBM modules mounted one in front of the other, were installed inside the pixel detector services on each side of the ATLAS interaction point at 90 cm < |z| < 111 cm, 3.2 < $|\eta|$ < 3.5 and at a radial distance from 5 cm to 7 cm from the center of the beam pipe. The modules have an inclination of 10° with respect to the ATLAS solenoid magnetic field direction to suppress erratic dark currents [19] in the diamonds. The DBM data-

acquisition system is shared with the ATLAS IBL [20]. After initial installment data were collected in the July 2015 run. These data have been analyzed and the first results of the DBM tracking capabilities are shown in Fig. 5. A clear separation between background particles from unpaired bunches and collision particles from colliding bunches is observed. After two electrical incidents in July 2015 with consequent loss of several modules, the DBM is now in re-commissioning phase.

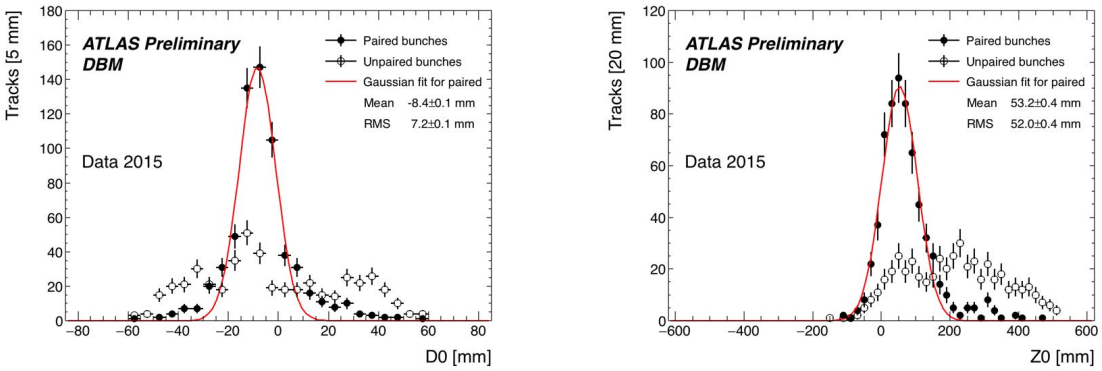

Figure 5: Radial distance (left plot) and longitudinal distance (right plot) of the closest approach of the projected particle tracks to the interaction point as recorded by a single DBM telescope with no alignment included yet.

6. Conclusion

The following milestones have recently been achieved: demonstration that the average signal pulse height of pCVD diamond detectors irradiated up to the dose of 5×10^{14} n/cm^2 does not depend on the the particle flux up to 10 MHz/cm^2; successful fabrication and operation of a pCVD diamond 3D detector where the average charge collected in a continuous fiducial region of cells is larger than the average charge collected in a planar detector on the same diamond by more than a factor of two and collected at a smaller bias voltage; the successful operation of the first pCVD diamond planar pixel device in an LHC experiment. In the future RD42 plans to study the pulse height dependence of CVD diamond sensors with pad and pixel electrodes and higher radiation doses up to 2×10^{16} n/cm^2 and also continue the development of 3D diamond detectors.

Acknowledgments

The RD42 Collaboration gratefully acknowledges the staff at CERN for test beam time and their help in setting up the excellent beam conditions. We would especially like to thank Henric Wilkins, the test beam coordinator, for his assistance in making our tests a success. We would also like to thank the beam line staff at the PSI High Intensity Proton Accelerator. We would especially like to thank Konrad Deiters, Manuel Schwarz and Davide Reggiani of PSI for their assistance in carrying out the diamond detector tests. We also extend our gratitude to Prof. Lin Li and David Whitehead of the University of Manchester Laser Processing Center for assisting in the production of the 3D diamond device. The research leading to these results received funding from

the European Union's Horizon 2020 research and innovation program under grant agreement No. 654168. This work was also partially supported by the Swiss National Science Foundation grant #20FL20_154216, ETH grant 51 15-1, Royal Society Grant UF120106 and the U.S. Department of Energy through grant DE-SC0010061.

References

[1] G. Apollinari , I. Bejar Alonso, O. Brüning, M. Lamont, L. Rossi (editors), *High-Luminosity Large Hadron Collider (HL-LHC): Preliminary Design Report*, **CERN-2015-005** 251 (2015).

[2] V. Cindro, *et al.*, *The ATLAS beam conditions monitor*, *JINST* **3(02):P02004** (2008).

[3] E. Castro, *et al.*, *The CMS beam conditions and radiation monitoring system*, *Physics Procedia* **37** (2012) 2097-2105.

[4] M. Domke, *et al.*, *Commissioning of the beam conditions monitor of the LHCb experiment at CERN*, *2008 IEEE Nuclear Science Symposium Conference Record* **N58-6, 3306** (2008).

[5] M. Barbero, *et al.*, *The FE-I4 pixel readout chip and the IBL module PoS(Vertex 2011)* **038** (2011).

[6] G. Aad, *et al.* [ATLAS collaboration], *The ATLAS experiment at the CERN Large Hadron Collider*, *JINST* **3 S08003** (2008).

[7] H. Kagan, M. Mikuz, W. Trischuk, *et al.*, *ATLAS Diamond Beam Monitor TDR*, *ATLAS Document DBM* **001** (2011).

[8] M. Červ, *et al.*, *The ATLAS Diamond Beam Monitor*, *JINST* **9 C02026** (2014).

[9] PSI High Intensity Proton Accelerator, *High Energy Beam Lines*, `http://www.psi.ch/abe/high-energy-beam-lines`

[10] R. Wallny, *et al.* [RD42 Collaboration], *Beam test results of the dependence of signal size on incident particle flux in diamond pixel and pad detectors*, *JINST* **10 C07009** (2015).

[11] D. Przyborowski, J. Kaplon, and P. Rymaszewski, *Design and Performance of the BCM1F Front End ASIC for the Beam Condition Monitoring System at the CMS Experiment*, *IEEE Trans. Nucl. Sci.*, **63**, 2300, (2016).

[12] The diamond material used in these tests was provided by II-VI Inc., 360 Saxonburg Road, Saxonburg, PA. `http://www.iiviinfrared.com/Optical-Materials/cvd-diamond_substrates.html`

[13] F. Bachmair, *CVD Diamond Sensors In Detectors For High Energy Physics*, *Ph.D. Thesis ETH Zurich*, (2016). `http://dx.doi.org/10.3929/ethz-a-010748643`

[14] H.Chr. Kästli, *et al.*, *Design and performance of the CMS pixel detector readout chip*, *Nucl. Instrum. Meth. A*, **565**, 188 (2006).

[15] S. Ritt, *DRS4 Evaluation Board*, `http://www.psi.ch/drs/evaluation-board`

[16] S. Parker, C. Kenney, J. Segal, *3D - A proposed new architecture for solid-state radiation detectors*, *Nucl. Instr. and Meth. A*, **395**, 328, (1997).

[17] F. Bachmair, *et al.* [RD42 Collaboration], *A 3D Diamond Detector for Particle Tracking*, *Nucl. Instrum. Meth. A*, **786**, 97 (2015).

[18] O. Toker, *et al.*, *VIKING, a CMOS low noise monolithic 128 channel frontend for Si-strip detector readout*, *Nucl. Instrum. Meth A*, **340**, 572 (1994).

[19] A.J. Edwards, *et al.*, *Radiation monitoring with diamond sensors in BABAR*, *IEEE Tran Nucl Sci* **51** (2004) 1808.

[20] F. Huegging, *et al.* [ATLAS Collaboration], *The ATLAS Pixel Insertable B-Layer (IBL)*, *Nucl. Instrum. & Meth. A* **650** 45 (2011).